VIP Nanostructure Growth

DOI: 10.1002/anie.200702001

A General Strategy for Synthesizing FePt Nanowires and Nanorods**

Chao Wang, Yanglong Hou, Jaemin Kim, and Shouheng Sun**

Synthesis of FePt nanoparticles with controlled shape and magnetic alignment has become an important goal in developing nanocrystal arrays for applications in information storage,[1] permanent-magnet nanocomposites,[2] and catalysis.[3] FePt alloys are chemically stable owing to the spin–orbit coupling and the hybridization between Fe 3d and Pt 5d states,[4] and their magnetic properties can be tuned by simply controlling the atomic ratio of Fe and Pt in the alloy structure. Recent syntheses have shown that spherical FePt nanoparticles are readily made by simultaneous reduction of platinum acetylacetonate ($[Pt(acac)_2]$) and thermal decomposition of iron pentacarbonyl ($[Fe(CO)_5]$).[1a,5] Thermal annealing results in hard magnetic FePt nanoparticle assemblies with coercivity reaching 30 kOe.[6] These small FePt nanoparticles are also very active in formic acid oxidation under fuel cell reaction conditions.[7] Despite these synthetic progresses, aligning these nanoparticles magnetically has constantly been a problem, and the magnetic easy axes of the nanocrystals in the assemblies are randomly oriented in three dimensions. Previous work on the synthesis and self-assembly of FePt nanocubes suggests that elongated nanocrystals may be used to achieve texture and magnetic alignment.[8] This controlled alignment of FePt nanoparticles is essential for the fabrication of single-particle recording media with ultrahigh density, magnetic nanocomposites with maximum energy product, and magnetotransport devices with optimum magnetoresistivity.

Herein we report a general strategy for synthesizing FePt nanowires (NWs) and nanorods (NRs). We refer to the one-dimensional nanostructures with a length of 100 nm or longer as NWs, and those below 100 nm as NRs. The diameters of both nanostructures are controlled to be 2–3 nm. The nanostructures were synthesized by reduction of $[Pt(acac)_2]$ and thermal decomposition of $[Fe(CO)_5]$ in a mixture of oleylamine (OAm) and octadecene (ODE) at 160 °C with the length readily tuneable. Our synthesis is fundamentally different from the very recent report on the preparation of FePt nanorods, for which the reaction was performed in oleic acid and oleylamine in a closed autoclave reaction system without stirring,[9] and offers much better control of both the dimensions and composition of the NWs/NRs. Owing to the structure confinement in the elongated shapes, these NWs and NRs show partial structural and magnetic alignment in thermally annealed self-assemblies. This study indicates that well-controlled NWs or NRs are likely the future choice for controlling texture and magnetic alignment in self-assembled nanomagnet arrays to support high-density magnetic information and as building blocks for fabricating highly sensitive magnetotransport devices.

The length control of the FePt NWs/NRs was realized by tuning the volume ratio of OAm/ODE, reaching from over 200 nm for NWs down to 20 nm for NRs. For example, FePt NWs with a length of over 200 nm were made when only OAm was used as both surfactant and solvent, while an OAm/ODE ratio of 3:1 gave FePt NWs of length 100 nm, and a 1:1 volume ratio of OAm/ODE led to FePt NRs of length 20 nm. Notably, using a greater proportion of ODE (OAm/ODE 1:3) led to the formation of spherical FePt nanoparticles of diameter 3 nm (see Figure S1 in the Supporting Information). With the amount of $[Pt(acac)_2]$ fixed (see the Experimental Section), the compositions of these FePt nanostructures were controlled by varying the amount of $[Fe(CO)_5]$ added to the reaction mixture and were measured by energy-dispersive spectroscopy (EDS). For example, for the FePt NWs of length 200 nm, using 0.15 mL $[Fe(CO)_5]$ led to about 55 % Fe in the final product, while using 0.1 mL $[Fe(CO)_5]$ yielded the product with about 45 % Fe. Note that CoPt NWs can also be made by reduction of $[Pt(acac)_2]$ and decomposition of $[Co_2(CO)_8]$ under similar reaction conditions (see Figure S2 in the Supporting Information).

Transmission electron microscope (TEM) images of the representative NWs and NRs are given in Figure 1. The images in Figure 1 a–c show NWs of length 200 nm and NRs of length 50 nm and 20 nm. The diameter of these NWs and NRs is about 2–3 nm. Figure 1 d is a high-resolution TEM (HRTEM) image of two single NWs of empirical formula $Fe_{55}Pt_{45}$. In one NW, the lattice fringes are oriented approximately 55° from the wire-growth direction. The interfringe distance was measured to be 0.214 nm, which is close to the lattice spacing of the (111) planes (0.22 nm) in the face-centered cubic (fcc) FePt structure. This result indicates that the [100] direction is parallel (or perpendicular) to the wire-growth direction, which is further confirmed by the image showing the lattice fringe in the second NW with clearly discernible (100) planes (0.198 nm interfringe spacing).

The synthesis and TEM analyses imply that OAm, a common organic surfactant, induces the one-dimensional growth of FePt under the current synthetic conditions. It is likely that OAm self-organizes into an elongated reverse-micelle-like structure within which the FePt nuclei are formed. This type of formation is similar to what has been proposed in the synthesis of Au NRs in the presence of

[*] C. Wang, Dr. Y. Hou, J. Kim, Prof. S. Sun
Department of Chemistry
Brown University
Providence, RI 02912 (USA)
Fax: (+1) 401-863-9046
E-mail: yanglong_hou@brown.edu
ssun@brown.edu

[**] This work was supported by NSF/DMR 0606264, INSIC, and ONR/MURI under grant no. N00014-05-1-0497.

Supporting information for this article is available on the WWW under http://www.angewandte.org or from the author.

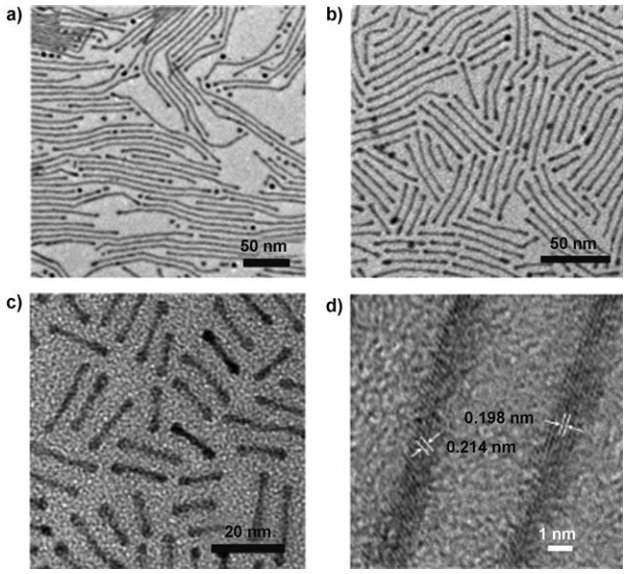

Figure 1. a–c) TEM images of $Fe_{55}Pt_{45}$ NWs and NRs with a length of 200 nm (a), 50 nm (b), and 20 nm (c). d) HRTEM image of portions of two single 50-nm $Fe_{55}Pt_{45}$ NWs.

cetyltrimethylammonium bromide (CTAB).[10] The elongated nuclei result in the different OAm packing densities on different surfaces, as indicated by (1), (2), and (3) in Figure 2a. In area (1), the molecules are well-organized and addition of FePt in this direction is more difficult owing to the presence of the hydrophobic barrier. Area (2) has less densely packed OAm and facilitates the growth of FePt along this direction and the formation of NWs or NRs. Area (3) is the most readily accessible place for the addition of FePt, leading to the fast growth of FePt and the rounded end of the NRs/NWs. The growth was monitored by taking aliquot reaction mixtures from oleylamine at 120°C after different reaction times, and the product was quickly precipitated out and redispersed into hexane for TEM analyses. In Figure 2b,c, TEM images are shown of the product obtained from the reaction mixtures. It can be concluded that small, thin rodlike

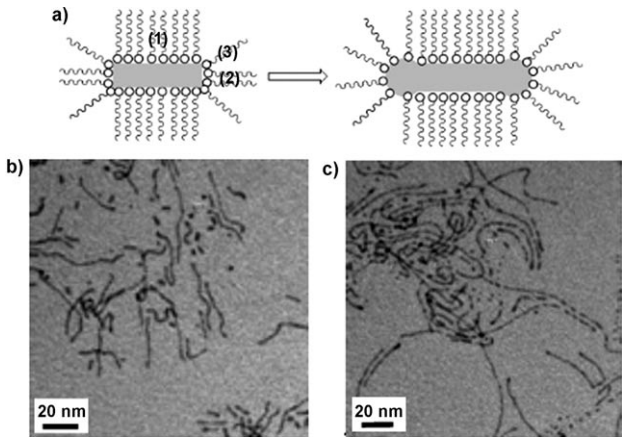

Figure 2. a) Schematic illustration of the growth of FePt NWs/NRs; b,c) TEM images of the FePt NRs/NWs obtained from the reaction in oleylamine at 120°C for 2 min and 5 min, respectively.

structures are initially present in the reaction medium and grow quickly into NWs/NRs. The fact that the growth in the [100] direction is controlled by the OAm/ODE ratio indicates that more OAm results in longer micellar structure and the formation of NWs, while dilution of OAm with ODE reduces the size of the structure, yielding NRs.

Controlled evaporation of the carrier solvent from the hexane dispersion of the 50-nm $Fe_{55}Pt_{45}$ NRs led to an $Fe_{55}Pt_{45}$ NR array with the NRs parallel to each other (Figure 3a). This assembly pattern is energetically favored as it gives the maximum van der Waals interaction energy arising from face–face interactions.[11] X-ray diffraction (XRD) of the as-synthesized NWs or NRs shows a fcc structure of FePt (Figure 3b). The broad peak originates from the small

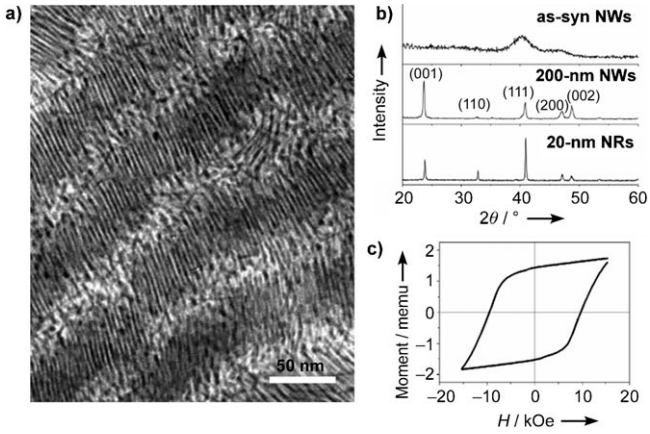

Figure 3. a) TEM image of self-assembled 50-nm FePt NRs; b) XRD pattern of the as-synthesized (as-syn; before thermal annealing) NWs, and 200-nm NWs and 20-nm NRs annealed in Ar at 750°C for 1 h; c) magnetic hysteresis loop of the 200-nm $Fe_{55}Pt_{45}$ NWs annealed in Ar at 750°C for 1 h. emu = electromagnetic unit.

diameter of the NWs or NRs (2–3 nm). Thermal annealing in an argon atmosphere at 750°C transforms the chemically disordered fcc structure of FePt to a chemically ordered face-centered tetragonal (fct) FePt structure, as shown by the XRD pattern in Figure 3b. More interestingly, the XRD pattern of the annealed 200-nm $Fe_{55}Pt_{45}$ NW assembly shows a much stronger (001) peak than the (111) peak or any other peaks, indicating a partial structural alignment with the (001) planes parallel to the substrate. The in-plane magnetic hysteresis loop of the assembly shows the better squareness with the coercivity reaching 9.5 kOe (Figure 3c). However, the annealed assembly of 20-nm $Fe_{55}Pt_{45}$ NRs (Figure 3b) shows the reduced alignment as evidenced by the intensity drop of the (001) peak. Furthermore, the XRD diffraction peaks for both NWs and NRs reveal a sharp decrease in the diffraction-peak width. This result indicates that both NWs and NRs are thermally unstable under the current annealing conditions, leading to the fusion of the nanostructures into larger aggregates. The NWs may be able to retain a larger portion of the elongated nanostructures and show better texture than the NRs do after the annealing process (Figure S3 in the Supporting Information). Our preliminary

test in NR stabilization by a MgO matrix revealed that the aggregation problem could be solved. Detailed studies on the controlled annealing and magnetic alignment in the self-assembled NR arrays are underway.

In conclusion, we report that controlled reduction of $[Pt(acac)_2]$ and decomposition of $[Fe(CO)_5]$ in a mixture of oleylamine and octadecene leads to a facile synthesis of FePt NWs and NRs with diameters of 2–3 nm. The length of the NWs/NRs is tunable from over 200 nm down to 20 nm by simply controlling the volume ratio of oleylamine/octadecene. The synthesis can also be extended to the preparation of CoPt NWs and NRs. With the structure confinement, these NWs or NRs may serve as unique building blocks for fabricating magnetically aligned nanomagnet arrays to support high-density magnetic information and to achieve highly sensitive magnetoresistive detection.

Experimental Section

Representative synthesis of FePt NWs and NRs: For the synthesis of 200-nm NWs, oleylamine (20 mL) was mixed with $[Pt(acac)_2]$ (0.2 g) at room temperature. Under a gentle nitrogen flow, the mixture was heated to 60 °C to form a light yellow solution. The solution was then heated to 120 °C in less than 5 min and kept at this temperature for 30 min. The color of the solution changed to dark yellow. $[Fe(CO)_5]$ (0.15 mL) was injected into the hot solution. The temperature was then raised to 160 °C. After 30 min, the solution was cooled down to room temperature by removing the heating mantle from the reaction flask. The NWs were separated by adding hexane (10 mL) and ethanol (50 mL) and subsequent centrifugation (6000 rpm). The product that was obtained was dispersed in hexane (10 mL).

Other NWs/NRs were synthesized under similar reaction conditions but with different volume ratios of oleylamine/octadecene. For example, 20-nm FePt NRs were made from 10 mL oleylamine and 10 mL octadecene.

Characterization: The FePt NWs/NRs were characterized with a transmission electron microscope (TEM, Philip EM 420 at 120 kV and JEOL 2010 at 200 kV). The Fe and Pt compositions were measured by energy-dispersive spectroscopy (EDS). X-ray powder diffraction patterns of the samples were collected on a Bruker AXS D8-Advanced diffractometer with $Cu_{K\alpha}$ radiation ($\lambda = 1.5418$ Å). Magnetic properties were measured with a Lakeshore 7404 high-sensitivity vibrating-sample magnetometer (VSM) with fields up to 1.5 T at room temperature. The nanoparticles were deposited from their hexane dispersions either on an amorphous carbon-coated copper grid for TEM image analyses or on a Si substrate for XRD and magnetic studies.

Received: May 5, 2007
Published online: June 22, 2007

Keywords: crystal growth · magnetic properties · nanostructures · transmission electron microscopy · X-ray diffraction

[1] a) S. Sun, C. B. Murray, D. Weller, L. Folks, A. Moser, *Science* **2000**, *287*, 1989; b) D. Weller, M. F. Doerner, *Annu. Rev. Mater. Sci.* **2000**, *30*, 611; c) A. Moser, K. Takano, D. T. Margulies, M. Albrecht, Y. Sonobe, Y. Ikeda, S. Sun, E. E. Fullerton, *J. Phys. D* **2002**, *35*, R157; d) I. R. McFadyen, E. E. Fullerton, M. J. Carey, *MRS Bull.* **2006**, *31*, 379; e) R. F. Service, *Science* **2006**, *314*, 1868; f) S. Sun, *Adv. Mater.* **2006**, *18*, 393; g) Y. F. Xu, M. L. Yan, D. J. Sellmyer, *J. Nanosci. Nanotechnol.* **2007**, *7*, 206.

[2] a) E. F. Kneller, R. Hawig, *IEEE Trans. Magn.* **1991**, *27*, 3588; b) R. Skomski, J. M. D. Coey, *Phys. Rev. B* **1993**, *48*, 15812; c) T. Schrefl, H. Kronmüller, J. Fidler, *J. Magn. Magn. Mater.* **1993**, *127*, L273; d) H. Zeng, J. Li, J. P. Liu, Z. L. Wang, S. Sun, *Nature* **2002**, *420*, 395; e) S. D. Bader, *Rev. Mod. Phys.* **2006**, *78*, 1.

[3] a) T. Toda, H. Igarashi, H. Uchida, M. Watanabe, *J. Electrochem. Soc.* **1999**, *146*, 3750; b) J. Jiang, A. Kucernak, *J. Electroanal. Chem.* **2002**, *520*, 64; c) E. Antolini, J. R. C. Salgado, E. R. Gonzalez, *J. Power Sources* **2006**, *160*, 957.

[4] a) T. Burkert, O. Eriksson, S. I. Simak, A. V. Ruban, B. Sanyal, L. Nordström, J. M. Wills, *Phys. Rev. B* **2005**, *71*, 134411; b) G. Brown, B. Kraczek, A. Janotti, T. C. Schulthess, G. M. Stocks, D. D. Johnson, *Phys. Rev. B* **2003**, *68*, 052405; c) O. Kitakami, S. Okamoto, N. Kikuchi, Y. Shimada, *Jpn. J. Appl. Phys.* **2003**, *42*, L455; d) J. B. Staunton, S. Ostanin, S. S. A. Razee, B. L. Gyorffy, L. Szunyogh, B. Ginatempo, E. Bruno, *Phys. Rev. Lett.* **2004**, *93*, 257204; e) C. Antoniak, J. Lindner, M. Spasova, D. Sudfeld, M. Acet, M. Farle, K. Fauth, U. Wiedwald, H.-G. Boven, P. Ziemann, F. Wilhelm, A. Rogalev, S. Sun, *Phys. Rev. Lett.* **2006**, *97*, 117201.

[5] a) S. Sun, E. E. Fullerton, D. Weller, C. B. Murray, *IEEE Trans. Magn.* **2001**, *37*, 1239; b) M. Chen, J. P. Liu, S. Sun, *J. Am. Chem. Soc.* **2004**, *126*, 8394; c) S. Momose, H. Kodama, T. Uzumaki, A. Tanaka, *Jpn. J. Appl. Phys.* **2005**, *44*, 1147.

[6] K. Elkins, D. Li, N. Poudyal, V. Nandwana, Z. Q. Jin, K. H. Chen, J. P. Liu, *J. Phys. D* **2005**, *38*, 2306.

[7] W. Chen, J. Kim, S. Sun, S. Chen, *Phys. Chem. Chem. Phys.* **2006**, *8*, 2779.

[8] M. Chen, J. Kim, J. P. Liu, H. Fan, S. Sun, *J. Am. Chem. Soc.* **2006**, *128*, 7132.

[9] M. Chen, T. Pica, Y. Jiang, P. Li, K. Yano, J. P. Liu, A. K. Datye, H. Fan, *J. Am. Chem. Soc.* **2007**, *129*, 6348.

[10] a) J. Gao, C. M. Bender, C. J. Murphy, *Langmuir* **2003**, *19*, 9065; b) L. Gou, C. J. Murphy, *Chem. Mater.* **2005**, *17*, 3668; c) I. Pastoriza-Santos, J. Pérez-Juste, L. M. Liz-Marzán, *Chem. Mater.* **2006**, *18*, 2465; d) P. Zijlstra, C. Bullen, J. W. M. Chon, M. Gu, *J. Phys. Chem. B* **2006**, *110*, 19315.

[11] a) C. Burda, X. Chen, R. Narayanan, M. A. El-Sayed, *Chem. Rev.* **2005**, *105*, 1025; b) S. Yamamuro, K. Sumiyama, *Chem. Phys. Lett.* **2006**, *418*, 166.

